JOURNAL OF MATERIALS SCIENCE 27 (1992) 3353–3358

Hardness and indentation-induced damage of SiC-coated graphite

CHIN-CHEN CHIU
Department of Metallurgy, Mechanics, and Materials Science, Michigan State University, East Lansing, Michigan 48824, USA

The hardness and indentation damage of chemical vapour-deposited SiC coating/graphite substrate composites have been studied. Experimental results indicate that hardness is a non-linear function of coating thickness, and is not significantly affected by the changes in the magnitude of the residual stresses in SiC coating. The size of indentation lateral crack, observed using optical microscopy, varies with coating thickness. Acoustic emission spectra show that thinner coatings suffer more extensive fracture as compared with thicker coatings.

1. Introduction

Hard coatings can be used as protective layers for substrates against erosive wear. In such applications, the knowledge of coating wear resistance, adherence, residual stress, and contact stress-induced damage becomes important for coating design. Indentation testing can be a guide to these coating properties [1–12]. Recently, some researchers [1–12] have paid attention to the theoretical analysis of indentation tests on coated materials. For example, Bhattacharya and Nix [11] studied the variation of hardness with coating thickness, according to an elastic and plastic deformation analysis. Jonsson and Hogmark [12] proposed load-shearing models to analyse the hardness of coated materials. However, indentation testing leads to a complex response in specimens beneath the indentation point, such as reversible elastic contact stress, irreversible plastic deformation, and indentation fracture. According to these authors, the theoretical work is still in the development stage and requires more experimentation.

The objective of the present work was to study experimentally the hardness and indentation damage of SiC coating/graphite substrate composites. Indentation testing was performed using the Vickers' indentation technique, accompanied by acoustic emission measurement. The indentation damage was observed using optical microscopy and scanning electron microscopy.

2. Experimental procedure

Chemical vapour-deposited SiC coating/graphite substrate composites were used in this experiment. The as-received billets were cut into specimens 5 cm × 0.8 cm × 0.5 cm, with coating on a single 5 cm × 0.8 cm surface. The uncoated surfaces of the graphite substrate were polished using 600 grit SiC polishing paper and the coated surface was polished using diamond paste (1 μm). The coating thickness was measured from cross-sectional area using an optical microscope.

Hardness was determined using the Vickers' indentation technique with a 70 μm s^{-1} loading speed, a 5 s indentation time, and loads of 9.8, 49 and 98 N. The hardness was calculated from [13]

$$H_* = \frac{P}{2a^2} \quad (1)$$

where P and a are load and half-diagonal of the indentation impression, respectively. Average hardness was calculated from at least ten indents. The indentation-induced lateral cracks could cause an interference fringe with reflected light. The radius of the fringe was measured using an optical microscope.

An acoustic emission processor (PAC 3000/3004, Physical Acoustics Corporation, Princeton, NJ) was used to detect the signal due to indentation fracture. The sensors were 150 kHz resonant transducers (PAC model R15), which were connected to the preamplifiers with 100–300 kHz band pass filters and 40 dB gain. The processor was set for an additional gain of 32 dB and the threshold voltage was 3 V. To receive the signal, the distance from sensors to indentation point was 1.2 ± 0.2 cm.

To examine the indentation damage further, the indented specimens were fractured by three-point bend loading, with the coated surface on the tensile side. The fracture surface was observed using a scanning electron microscope (SEM). In addition, the indented specimens were heated in air in an electric furnace at 550 °C until the graphite substrates were totally removed by oxidation in order to obtain monolithic coating layers alone. The coating layers were carefully set in an ultrasonic cleaner for 2 min to remove the oxidation ash of graphite, and then they were observed using an optical microscope.

Previous work has showed that the residual stresses in the SiC coating were a function of the ratio of graphite substrate thickness to coating thickness [14]. To investigate the effect of coating's residual stress on indentation damage, indentation was repeatedly performed while the graphite substrate, with a constant coating thickness, was polished off step by step. The

0022–2461

minimum residual substrate thickness was > 1 mm, to avoid disturbance of the contact stress field caused by the substrate thickness change.

3. Results and discussion

3.1. Hardness

Fig. 1 illustrates the relationships between the hardness, coating thickness, and indentation loads. Monolithic graphite substrate (without coating) corresponds to a hardness of $H_s = 0.28$ GPa. The initial increase in coating thickness does not apparently increase the hardness of coated graphite substrate until the thickness approaches a certain range. Beyond this range, the coating effectively insulates the indentation stress field from the substrate. Thus, the indentor does not "feel" the existence of the substrate and the hardness converges to a limiting value. The limiting values under indentation loads of 9.8 and 49 N correspond to $H_c = 34.8$ and 33.0 GPa, respectively. The variation of hardness with coating thickness qualitatively agrees with the results reported by Kamata *et al.* [3].

From elastic and plastic theory and finite element calculation, Bhattacharya and Nix [11] proposed an empirical equation for the hardness of hard coating/soft substrate composites, H_*, namely

$$\frac{H_* - H_s}{H_c - H_s} = \exp\left[- \frac{(H_c/H_s)(t_*/t_c)}{(\sigma_c/\sigma_s)(E_c/E_s)^{1/2}} \right] \quad (2)$$

where the subscripts c and s refer to the properties of the coating and the substrate, respectively. H, E, σ, and t are hardness, elastic modulus, yield strength, and thickness, respectively. t_* is the indentation impression depth. For a Vickers' indentation impression, t_* is given by

$$t_* = a\frac{\cot(68°)}{2^{1/2}} \quad (3)$$

Combining Equations 1 and 3 yields

$$t_* = \left[\frac{P}{4H_*}\right]^{1/2} \cot(68°) \quad (4)$$

Substituting Equation 4 into Equation 2 and then taking natural logarithms twice on Equation 2 yields

$$\ln\left[- \ln\left(\frac{H_* - H_s}{H_c - H_s}\right)\right] = 0.5 \ln\left(\frac{P}{H_* t_c^2}\right) + C \quad (5)$$

where

$$C = \ln\left[\frac{(H_c/H_s)\cot(68°)}{2(\sigma_c/\sigma_s)(E_c/E_s)^{1/2}}\right]$$

Equation 5 has the form of $Y = 0.5\ X + C$. As C is constant, a linear relationship between X and Y is expected. However, the experimental data (Fig. 2) indicate that X and Y do not exhibit a linearly proportional relationship. Thus, Equation 2 is not suitable for the SiC coating/graphite substrate composites. Bhattacharya and Nix [11] did not consider strain hardening or cracking in Equation 2. For brittle coatings and/or substrates, indentation can involve not only elastic and plastic deformation but also indentation-induced fracture. The complexity of indentation fracture is one of the important factors accounting for the non-linear relationship.

Jonsson and Hogmark [12] also proposed empirical equations indicating the development of hardness, H_*, with coating thickness, t_c. Equation 5 of [12] deduces that the hardness of substrate and coating are the same when t_c approaches infinity. Unfortunately, the result does not make physical sense.

3.2. Acoustic emission

Acoustic emission (AE) measurement is one of the useful techniques to provide information of the cracking beneath an indentation point. Fig. 3a is a spectrum of AE event versus amplitude distribution in one indentation test. In all AE measurements, about 85% and 15% of AE events are acquired during loading and unloading procedures, respectively. The amplitude distribution usually ranges from 60–95 dB. The total AE events, reflecting the degree of indentation fracture [15], are non-linear functions of coating thickness (Fig. 3b). A monolithic graphite substrate (without coating) corresponds to a smal number of AE events. Thinner coatings yield more AE events as compared with thicker coatings. However, AE

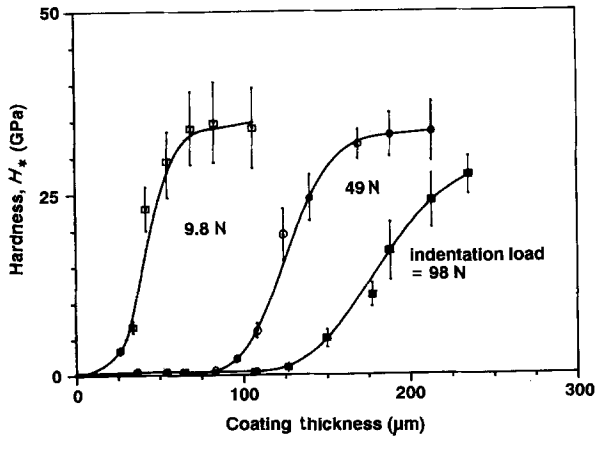

Figure 1 Variation of the observed hardness with SiC coating thickness. The error bar represents two standard deviations.

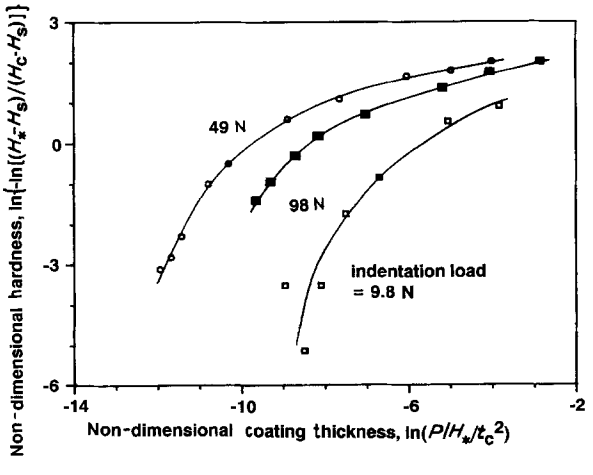

Figure 2 A plot of non-dimensional hardness and non-dimensional coating thickness.

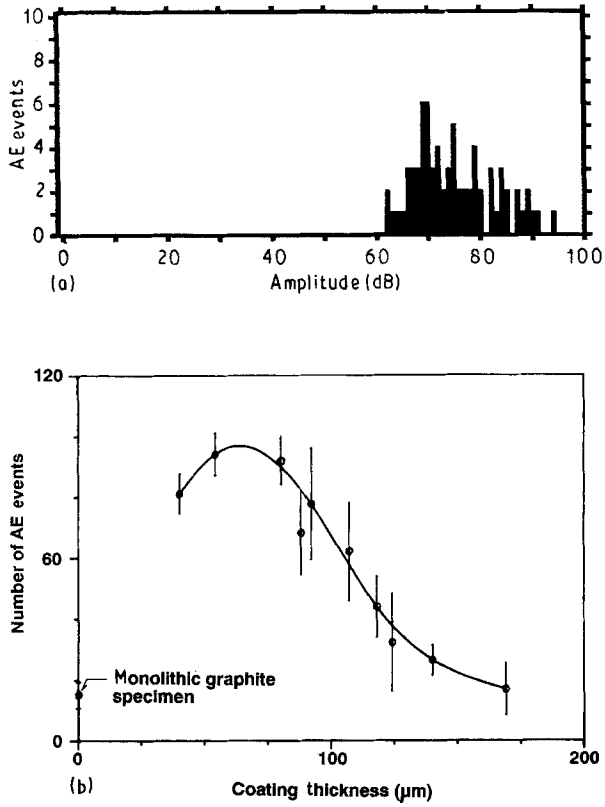

Figure 3 (a) An acoustic emission spectrum in one indentation test. (b) Variation of AE events with coating thickness, under a 49 N indentation load.

measurement cannot explain the morphological development of indentation fracture. Thus, AE signal analysis should cooperate with indentation damage observations.

3.3. Indentation damage observations

Fig. 4a is an optical micrograph of an indentation impression. Because the SiC coating is translucent, the interference fringe caused by lateral cracks can be seen through reflected light using an optical microscope with a suitable filter (see Fig. 4a and b). The lateral crack radius is a function of coating thickness and indentation load (Fig. 5). For example, the crack radius related to 49 N indentation loading initially increases with increasing coating thickness, and then reaches a maximum value at $t_c \approx 88$ μm. As the coating thickness further increases, the crack radius decreases. Finally, the interference fringe of $t_c \geqslant 170$ μm cannot be clearly seen through optical microscopy.

Radial cracks were observed in some indented specimens (such as Fig. 4a). In contrast to the lateral crack, the radial cracks did not exhibit regular development in the length, number, and propagation direction. With increasing loading or with decreasing coating thickness, the pattern of radial cracks was less reproducible and reliable.

To observe indentation damage further, monolithic SiC coating layers were prepared by totally removing the graphite substrate from indented specimens. The translucent SiC layers were then examined using transmitted light. Because extensive indentation damage occurred, thick SiC coating layers developed

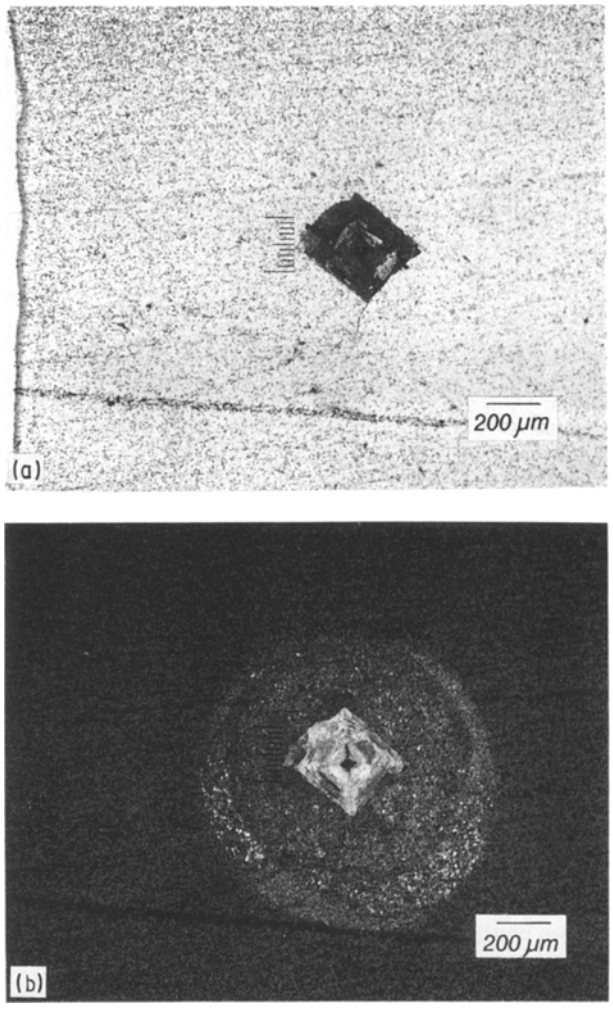

Figure 4 (a) An optical micrograph of an indentation impression. (b) Interference fringe caused by the lateral cracks in the SiC coating layer.

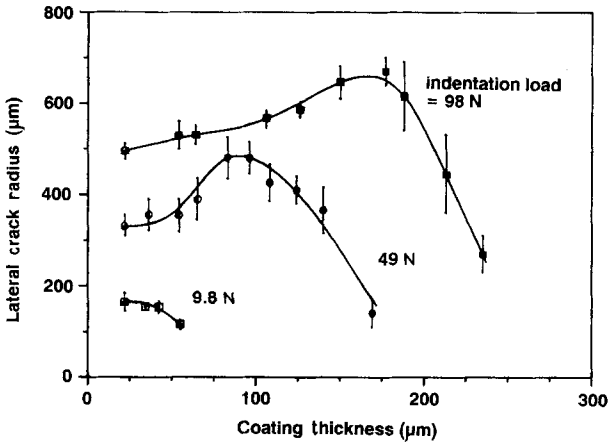

Figure 5 Influence of coating thickness on lateral crack radius. The graphite substrate thickness ≈ 5 mm.

a dark spot at the loading point, in addition to a surrounding fringe of lateral cracks (Fig. 6a). However, the damage caused a through hole in the centre of thinner SiC layers (Fig. 6b). A comparison of Figs 4b, 6a and b shows that the indentation-induced lateral cracks develop in the SiC layer, rather than at the coating/substrate interface, otherwise, the monolithic SiC layer would not have a lateral crack interference

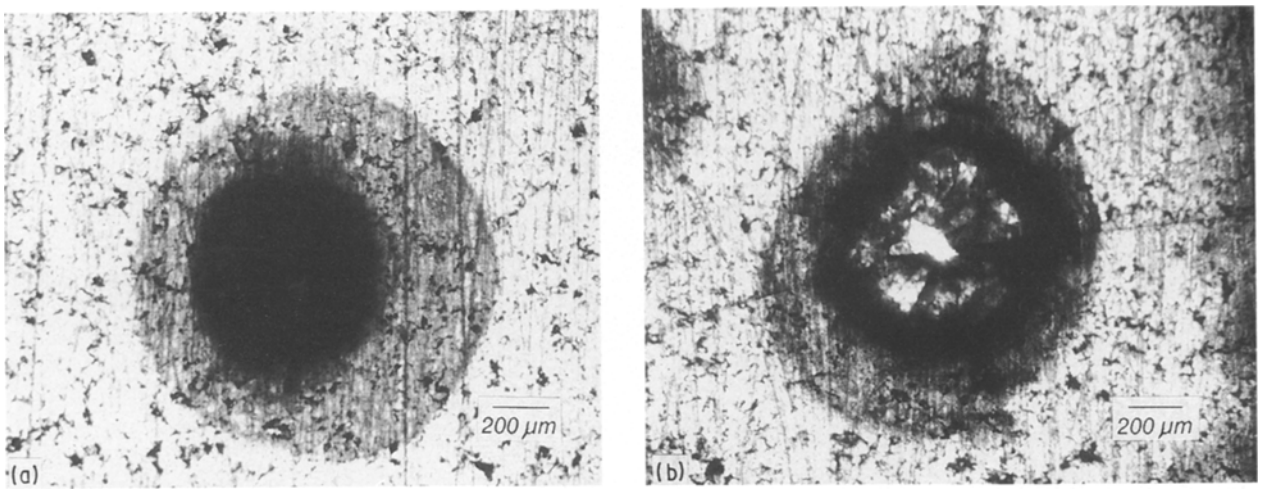

Figure 6 Optical micrographs of translucent SiC coating layers. (a) $P = 98$ N and $t_c = 150$ μm, (b) $P = 98$ N and $t_c = 68$ μm. The pictures were not clear because of being taken through transmitted light.

fringe. Some researchers [6–9] proposed that an indentation-induced debonding test could be useful in measuring the coating adherence. Because the SiC coating/graphite substrate composites have a great interfacial strength, the debonding test is useless in the present study.

Fig. 7 shows scanning electron micrographs of the fracture surface of indented specimens. When the coating is thick, indentation damage only occurs in the small region beneath the indentation point (Fig. 7a). As the coating thickness decreases, the damaged region under a constant indentation loading becomes large (Fig. 7b and c). The lateral cracks grow radially and the damaged region becomes deeper. For constant coating thickness, the lateral crack radius and damaged region increase with increasing indentation load (Fig. 7b and c). These scanning electron micrographs indicate that the graphite substrate is seemingly not cracked.

According to the hardness and AE measurements, as well as SEM and optical microscopy observations, we outline the indentation damage development with respect to coating thickness as shown in Fig. 8. The patterns for a 49 N indentation load and 40 μm $\leqslant$ $t_c \leqslant$ 200 μm are explained as follows.

(a) Thinner coatings correspond to a larger indentation impression area from which the hardness is calculated. Lateral cracks do not significantly extend out and the interference fringe is restricted to the impression area (Fig. 8a).

(b) As the coating thickness increases, the lateral crack radius increases. In contrast, the impression

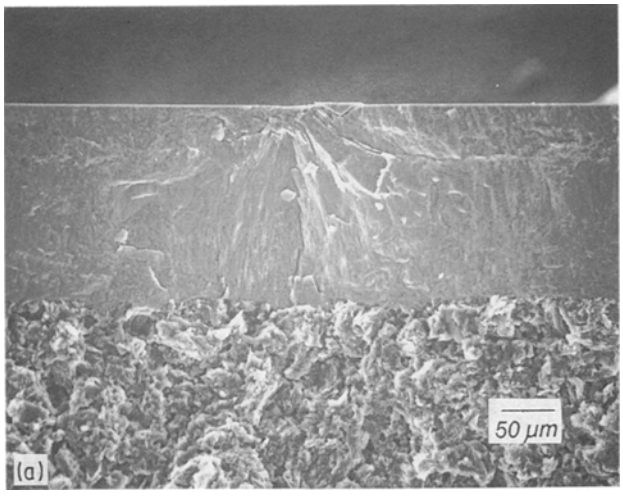

Figure 7 Scanning electron micrographs of the fracture surface of indented specimens. (a) $P = 49$ N and $t_c = 180$ μm, (b) $P = 49$ N and $t_c = 120$ μm, (c) $P = 98$ N and $t_c = 120$ μm.

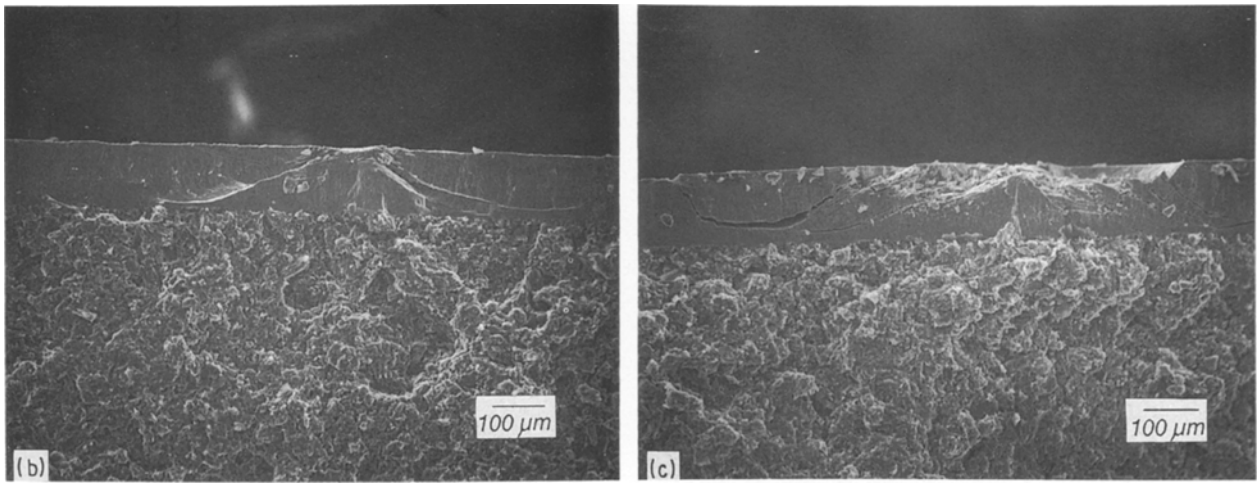

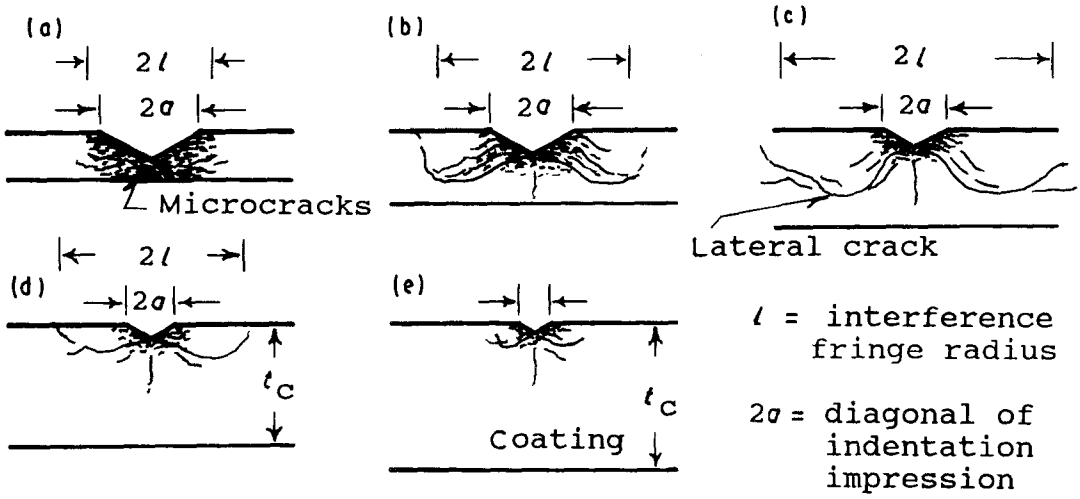

Figure 8 Schematic drawings showing the effect of coating thickness on indentation damage. Indentation impression area and indentation fracture gradually decrease from (a) to (e). Interference fringe radius increases from (a) to (c); however, it decreases from (c) to (d). Maximum fringe radius occurs in (c). The fringe in (e) cannot be clearly observed through optical microscopy.

area and the indentation fracture gradually decrease (Fig. 8a–c).

(c) When the coating thickness is equal to a certain value, the lateral crack radius reaches a maximum value. However, the impression area and the indentation fracture still decrease (Fig. 8c).

(d) The impression area, indentation fracture, and lateral crack radius decrease with further increase of coating thickness. Finally, the lateral crack interference fringe cannot be clearly seen through optical microscopy. The indentation damage only occurs in the small region beneath the indentation point (Fig. 8c–e).

3.4. Residual stress effect

A previous study indicated that the elastic modulus of the SiC coating and graphite substrate are $E_c = 359$ GPa and $E_s = 9.9$ GPa [14]. The residual stresses in the SiC coating are compressive and are a decreasing function of the ratio of substrate thickness to coating thickness, R (Fig. 9). In order to investigate the effect of the coating's residual stress on indentation damage, the graphite substrate was polished off step by step during the repeated indentation test. The minimum residual substrate thickness was > 1 mm and the coating thickness was constant.

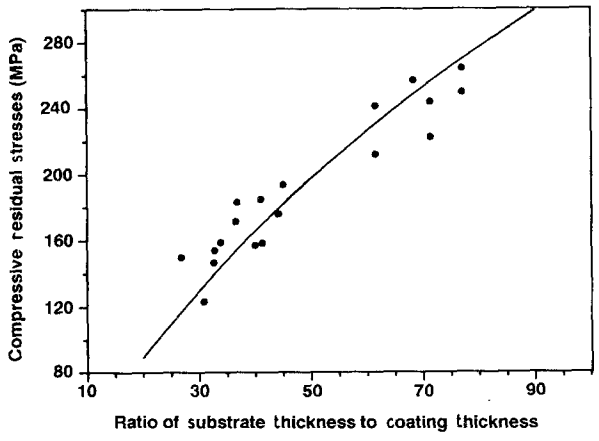

Figure 9 Variation of the coating's residual stress with the ratio of substrate thickness to coating thickness (after [14]).

Fig. 10a indicates that the hardness (49 N indentation load) does not significantly vary for a residual stress decrease from about 250 MPa to 80 MPa. The experimental results make physical sense if we qualitatively compare the indentation stress field with the magnitude of the coating's residual stress. Lawn and Swain [16] plotted a stress profile of a semi-infinite body under a concentrated load (Boussinesq's problem). Other researchers [17–19] also proposed stress profiles for the contact stress analysis of a layered elastic solid. As shown in those stress profiles [16–19], the stress concentration beneath the loading point is large so that the plastic deformation in practical indentation testing is unavoidable. However, the residual stresses in coatings, attributed to the restricted elastic deformation, is minor in comparison with the indentation stress. Thus, the effect of residual stress on the hardness can be insignificant.

Fig. 10b shows that the specimens wth $t_c = 124$ and 65 μm exhibit no obvious change of lateral crack radius with residual stress decrease. However, the specimens with $t_c = 88$ μm exhibit a decreasing crack radius. The apparent residual stress effect for specimens with intermediate coating thickness is reasonable, which can be explained from the spatial distribution of the indentation stress field. As proposed in the previous paragraph, stress concentration occurs beneath the loading point so that the coating's residual stress is not significant to the indentation damage immediately beneath the loading point. However, the indentation stress intensity diminishes with the increasing distance from the loading point [16–19]. The coating's residual stress finally becomes predominant in the domain far from the loading point. Fig. 5 indicates that specimens with $t_c \approx 88$ μm have the greatest lateral crack radius (49 N indentation load). The corresponding crack tip could extend to the domain where the residual stress is predominant. Consequently, the size of the lateral crack is substantially affected by the changes in the magnitude of the coating's residual stress. In contrast, the specimens with

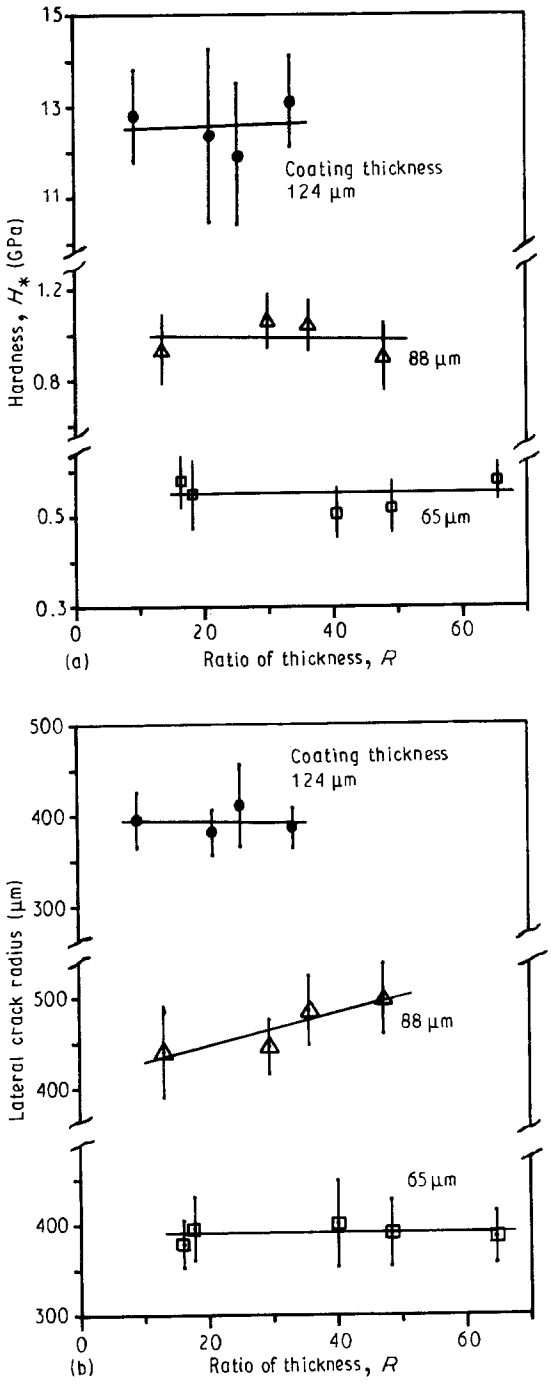

Figure 10 Variation of indentation damage with the ratio of substrate thickness to coating thickness: (a) hardness, (b) lateral crack radius. The linear regression lines were calculated using the least squares method.

t_c = 124 and 65 μm have a smaller lateral crack radius (Fig. 5). The crack tip is closer to the loading point and could still be located in the domain where the indentation stress field is predominant. As a result, the effect of the coating's residual stress change on lateral crack radius could be negligible.

4. Conclusions

The SiC coating/graphite substrate composite is representative of a soft substrate deposited with a hard coating. Indentation testing has given the following experimental results.

1. The hardness under a constant indentation load non-linearly increased with increasing coating thickness and then reached a limiting value.
2. The indentation test induced cracks and acoustic emission signals. Thinner coatings suffered more extensive indentation fracture in comparison with thicker coatings.
3. Lateral cracks occur in the SiC coating, rather than at the coating/substrate interface. The lateral crack radius under a constant load varied with coating thickness.
4. The changes in the magnitude of the coating's residual stress did not significantly affect the hardness. However, the specimens with intermediate coating thickness exhibited a decreasing lateral crack radius with residual stress decrease.

Acknowledgement

The author thanks Michael. B. Miller, Material Technology Corporation, Dallas, Texas, for providing the SiC coating/graphite substrate composites.

References

1. B. R. LAWN and E. R. FULLER, *J. Mater. Sci.* **19** (1984) 4061.
2. M. F. GRUNINGER, B. R. LAWN and E. N. FARABAUGH, *J. Amer. Ceram. Soc.* **70** (1987) 344.
3. K. KAMATA, N. AIZAWA and M. MORIYAMA, *J. Mater. Sci. Lett.* **5** (1986) 1055.
4. P. H. KOBRIN and A. B. HARKER, *J. Mater. Sci.* **24** (1989) 1363.
5. R. B. KING, *Int. J. Solids Struct.* **23** (1987) 1657.
6. A. G. EVANS and J. W. HUTCHINSON, *ibid.* **20** (1984) 455.
7. C. ROSSINGTON, A. G. EVANS, D. B. MARSHALL and B. T. K. YAKUB, *J. Appl. Phys.* **56** (1984) 2639.
8. J. E. RITTER, T. J. LARDNER, L. G. ROSENFELD and M. R. LIN, *ibid.* **66** (1989) 3626.
9. L. G. ROSENFELD, J. E. RITTER, T. J. LARDNER and M. R. LIN, *ibid.* **67** (1990) 3291.
10. V. R. HOWES and M. A. RYAN, *J. Austral. Ceram. Soc.* **22** (1986) 13.
11. A. K. BHATTACHARYA and W. D. NIX, *Int. J. Solids Struct.* **24** (1988) 1287.
12. B. JONSSON and S. HOGMARK, *Thin Solid Films* **114** (1984) 257.
13. G. R. ANSTIS, P. CHANTIKUL, B. R. LAWN and D. B. MARSHALL, *J. Amer. Ceram. Soc.* **64** (1981) 533.
14. C. C. CHIU, *ibid* **64** (1990) 1999.
15. R. D. RAWLINGS, in "Surface Coatings-2" (Elsevier Applied Science, New York, 1988) p. 71.
16. B. R. LAWN and M. V. SWAIN, *J. Mater. Sci.* **10** (1975) 113.
17. R. B. KING and T. C. O'SULLIVAN, *Int. J. Solids Struct.* **23** (1987) 581.
18. P. K. GUPTA and J. A. WALOWIT, *Trans ASME, J. Lub. Tech.* **96** (1974) 250.
19. W. T. CHEN and P. A. ENGEL, *Int. J. Solids Struct.* **8** (1972) 1257.

Received 13 March
and accepted 1 July 1991